

# Heterodyne-Detected Ultrafast X-Ray Diffraction and Scattering from Nonstationary States

Kochise Bennett<sup>a,b,\*</sup>, Markus Kowalewski<sup>a</sup>, and Shaul Mukamel<sup>a,b†</sup>

<sup>a</sup>*Chemistry Department, University of California, Irvine, California 92697-2025, USA and*

<sup>b</sup>*Department of Physics and Astronomy, University of California, Irvine, California 92697-2025, USA*

(Dated: July 31, 2018)

Free-electron laser hard X-ray light sources can provide high fluence, femtosecond pulses, enabling the time-resolved probing of structural dynamics and elementary relaxation processes in molecules. Traditional X-ray elastic scattering from crystals in the ground state consists of sharp Bragg diffraction peaks that arise from pairs of molecules and reveal the ground state charge density. Scattering of ultrashort X-ray pulses from gases, liquids, and even single molecules is more complex and involves both single- and two- molecule contributions, diffuse (non-Bragg) features, elastic and inelastic components, contributions of electronic coherences in nonstationary states, and interferences between scattering off different states (heterodyne detection). We present a unified description that covers all these processes and discuss their relative magnitudes for gas-phase NaI. Conditions for the observation of holographic (heterodyne) interference, which has been recently discussed [1], are clarified.

The term diffraction refers to the off-resonant elastic scattering of light [2–4]. From a simple, classical picture, the amplitude of the light scattered from each location in the material acquires a spatial phase-factor and repeated spatial patterns lead to Bragg peaks in the scattered signal where the light scattered from different points in the sample adds coherently. This technique has been used for over a century to probe the structure of crystals and has been extended to diffuse scattering from liquids, probing nearest-neighbor distances and served as inspiration for similar the conceptually similar electron diffraction technique [5, 6]. More recently, effort has been made to push diffraction to the single-molecule limit, eliminating the need for time-consuming crystal preparation [7–11]. Time-resolved X-ray diffraction is a natural way to track the structural changes that characterize phase transitions and chemical reactions and has been actively pursued to create molecular movies [6, 12–21]. These efforts have been made possible by the development of free-electron hard X-ray sources capable of producing bright, femtosecond-duration pulses [22–27].

Heterodyne detection involves the interference of a weak optical signal field with a strong reference (local oscillator). The resulting signal is linear (rather than quadratic) in the weaker signal field and thus scales favorably in addition to revealing phase information. Such holographic detection is well established in the visible regime and has been extended to transient X-ray diffraction in crystals and powders [28, 29] and was recently discussed in the gas phase [1]. For weak excitations, where only a small fraction of the molecules is excited, the signal from the ground state molecules serves as a local oscillator for the weaker excited state signal. An external local oscillator is not needed since it is generated *in situ*. This amounts to self-heterodyne detection.

X-ray diffraction from crystals in the ground state is purely elastic, contains no electronic coherence, and

is given by a product of scattering amplitudes of two molecules. Time-resolved scattering from photoexcited molecules in the gas phase, in contrast, is a sum of single-molecule contributions, contains elastic and inelastic contributions, and can depend on electronic coherence. We calculate the X-ray scattering by an ensemble of molecules prepared in a superposition of valence electronic states and identify the various contributions and show that, in the absence of valence electronic coherence and inelastic X-ray scattering, the gas-phase diffraction signal is simply given by the sum of ground- and excited-state contributions and contains no cross (heterodyne) terms.

The total charge-density operator for a system composed of molecules can be written as a sum of the charge densities from each molecule

$$\hat{\sigma}_T(\mathbf{r}) = \sum_{\alpha} \hat{\sigma}_{\alpha}(\mathbf{r} - \mathbf{r}_{\alpha}) = \sum_{\alpha} \int d\mathbf{q} e^{i\mathbf{q} \cdot (\mathbf{r} - \mathbf{r}_{\alpha})} \hat{\sigma}_{\alpha}(\mathbf{q}) \quad (1)$$

where  $\mathbf{r}_{\alpha}$  is the center of molecule  $\alpha$ . For a sufficiently dilute system such that the molecules have non-overlapping charge distributions, this separation is exact since each electron (the fundamental X-ray scatterer) can be rigorously assigned to a specific molecule. More generally, there will ordinarily be very little intermolecular electron density and this separation is justified. For identical molecules, the charge density operators of each molecule differ only by the spatial phase-factor associated with the location of the molecule and we may drop the  $\alpha$  subscript. Elastic light scattering comes proportional to the Thomson scattering cross section which gives the intensity distribution of free-electron scattering [2, 3]. Neglecting this and other pre-factors, the diffraction signal from a system initially in the ground state  $|g\rangle$  is

$$S(\mathbf{q}) = |\sigma_{gg}(\mathbf{q})|^2, \quad (2)$$

where  $\sigma_{gg}(\mathbf{q}) = \langle g | \hat{\sigma}(\mathbf{q}) | g \rangle$  is the ground state charge density in  $\mathbf{q}$ -space where  $\mathbf{q}$  is the momentum transfer. Equa-

tion (2) assumes that the scattering is elastic. In a previous work [30], we derived expressions for 1-molecule and 2-molecule contributions to frequency-resolved diffraction which we denote as  $S_1$  and  $S_2$  respectively [31]. In the supplementary information, we integrate out this frequency-resolution and take a quasi-elastic limit to arrive at the following simpler formulas

$$S_2(\mathbf{q}, t) = F(\mathbf{q}) \int dt |E_p(t)|^2 |\langle \hat{\sigma}(\mathbf{q}, t) \rangle|^2 \quad (3)$$

$$S_1(\mathbf{q}, t) = N \int dt |E_p(t)|^2 \langle |\hat{\sigma}(\mathbf{q}, t)|^2 \rangle \quad (4)$$

where  $E_p(t)$  is the temporal envelope of the X-ray pulse,  $\langle \dots \rangle$  stands for expectation value over the nuclear and electronic states, and the function

$$F(\mathbf{q}) = \sum_{\alpha} \sum_{\beta \neq \alpha} e^{-i\mathbf{q} \cdot (\mathbf{r}_{\alpha} - \mathbf{r}_{\beta})} \quad (5)$$

is known as the structure factor and encodes the long-range (intermolecular) order of the sample, the intramolecular structure being encoded in the  $\hat{\sigma}$ . Note the subtle distinction between these two expressions: Eq. (3) comes with  $|\langle \hat{\sigma}(\mathbf{q}) \rangle|^2$  while Eq. (4) comes with  $\langle |\hat{\sigma}(\mathbf{q})|^2 \rangle$ . The former coincides with the classical definition of diffraction (Eq. (2)) but is actually due to the coherent addition of the scattering amplitude from pairs of molecules while the latter accounts for single-molecule diffraction. In a crystal, the long-range order gives rise to sharp Bragg peaks in  $F(\mathbf{q})$  while the 1-molecule terms form a diffuse background that can be neglected. The enhancement at these Bragg peaks scales quadratically in the molecule number (i.e.,  $\propto N^2$ ) and the intensity at each peak comes proportional to the  $\mathbf{q}$ -space charge density at that point. This is the traditional picture of diffraction. Sampling the molecular  $\mathbf{q}$ -space charge density at the Bragg peaks is sufficient to reconstruct the magnitude of the  $\mathbf{q}$ -space charge density. By considering the diffuse scattering between Bragg peaks, enough information can be obtained to reconstruct the phase as well, providing one solution to the phase problem in X-ray diffraction *via* oversampling [32–34].

In the continuum limit, we can replace the summations over molecules with spatial integrations. Assuming spatial homogeneity (no long-range order), we obtain  $S_2 \propto \delta(\mathbf{q})$  and the 2-molecule terms contribute only at zero momentum transfer (the central maximum of the diffraction pattern) and the 1-molecule term becomes dominant. Thus, in the absence of long-range order, such as in a gas, the diffraction signal should be simulated with Eq. (4) rather than (3). It is a common error to write

the single-molecule diffraction as Eq. (4) but with  $|\langle \hat{\sigma} \rangle|^2$  rather than  $\langle |\hat{\sigma}|^2 \rangle$ . When all molecules in the sample are in the ground state and inelasticities are ignored, these two are the same, both being  $|\sigma_{gg}(\mathbf{q})|^2$ . More generally however, they result in different types of terms that,

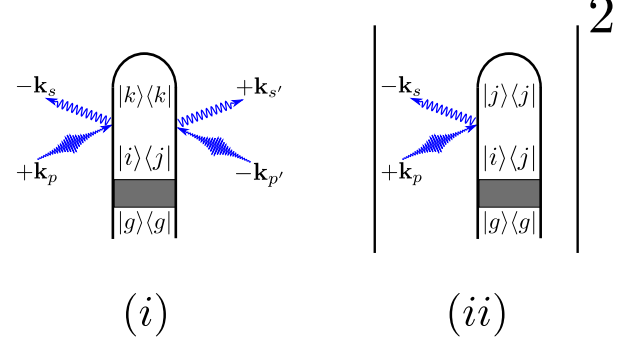


FIG. 1. Loop diagrams for single-molecule (i) and two-molecule (ii) X-ray scattering processes. The amplitude-squared form of the two-molecule contribution has been explicitly indicated. The shaded area represents an excitation process that prepares the system in an arbitrary superposition state ( $|g\rangle$  is the electronic ground state). We denote modes of the X-ray pulse with  $p$  and  $p'$  whereas  $s, s'$  represent relevant scattering modes ( $\mathbf{k}_{p(s)}$  has frequency  $\omega_{p(s)}$  and  $\mathbf{k}_{s(s')}$  has frequency  $\omega_{s(s')}$ ). Note that we use  $|\phi_i\rangle \rightarrow |i\rangle$  for the electronic states in this figure to aid readability. A complete list of diagrams is given Fig. (S1).

as will be shown next, affect the interpretation of the diffraction signal from nonstationary states.

We consider a molecular model consisting of two electronic states  $e, g$  and a single active nuclear coordinate  $\mathbf{R}$ . The time-dependent wavefunction of each molecule in the ensemble will be expanded in the product space

$$|\Psi(t)\rangle = e^{-i\hat{H}_0 t} \sum_{i=e,g} c_i(0) |\chi_i(0)\rangle \otimes |\phi_i\rangle \quad (6)$$

where  $|\chi_i\rangle$  is the (normalized) nuclear wavepacket on electronic state  $|\phi_i\rangle$ ,  $c_i$  is the electronic state amplitude, and  $\hat{H}_0$  is the field-free nuclear Hamiltonian. For a weak excitation, we will have  $|c_e|^2 = \epsilon \ll 1$  and  $\sum_i |c_i|^2 = 1$ . We treat the system in the Born-Oppenheimer approximation (BOA) wherein the nuclear wavepackets on each electronic eigenstate evolve independently and the Hamiltonian separates into the sum of kinetic and potential energies on each  $|\phi_i\rangle$ .

Explicitly expanding the results given in the supplement in the electronic states gives

$$S_1(\mathbf{q}, t) = N \left\{ \rho_{gg}(t) \langle \chi_g(t) | \hat{\sigma}_{gg}^\dagger(\mathbf{q}) \hat{\sigma}_{gg}(\mathbf{q}) | \chi_g(t) \rangle + \rho_{ge}(t) \langle \chi_g(t) | \hat{\sigma}_{ge}^\dagger(\mathbf{q}) \hat{\sigma}_{ge}(\mathbf{q}) | \chi_g(t) \rangle + \rho_{ee}(t) \langle \chi_e(t) | \hat{\sigma}_{ee}^\dagger(\mathbf{q}) \hat{\sigma}_{ee}(\mathbf{q}) | \chi_e(t) \rangle + \rho_{eg}(t) \langle \chi_e(t) | \hat{\sigma}_{eg}^\dagger(\mathbf{q}) \hat{\sigma}_{eg}(\mathbf{q}) | \chi_e(t) \rangle \right. \\ \left. + 2\Re[\rho_{eg}(t) \langle \chi_e(t) | \hat{\sigma}_{ee}^\dagger(\mathbf{q}) \hat{\sigma}_{eg}(\mathbf{q}) | \chi_g(t) \rangle + \rho_{eg}(t) \langle \chi_g(t) | \hat{\sigma}_{eg}^\dagger(\mathbf{q}) \hat{\sigma}_{ee}(\mathbf{q}) | \chi_e(t) \rangle] \right\} \quad (7)$$

$$S_2(\mathbf{q}, t) = F(\mathbf{q}) \left| \rho_{gg}(t) \langle \chi_g(t) | \hat{\sigma}_{gg}(\mathbf{q}) | \chi_g(t) \rangle + \rho_{ee}(t) \langle \chi_e(t) | \hat{\sigma}_{ee}(\mathbf{q}) | \chi_e(t) \rangle + 2\Re[\rho_{eg}(t) \langle \chi_e(t) | \hat{\sigma}_{eg}(\mathbf{q}) | \chi_g(t) \rangle] \right|^2. \quad (8)$$

where the electronic populations and coherences are given by the diagonal and off-diagonal elements of the density matrix  $\rho_{ij}(t) = c_i^*(t)c_j(t)$  and we have defined the electronic-state matrix elements of the charge-density operator  $\hat{\sigma}_{ij}(\mathbf{q}) = \langle \phi_i | \hat{\sigma}(\mathbf{q}) | \phi_j \rangle$  (which remains an operator in the nuclear space) and, for brevity, omitted the time integration over the X-ray pulse envelope.

The first four terms on the right-hand side of Eq. (7) represent the elastic ( $\sigma_{gg}$  and  $\sigma_{ee}$ ) and inelastic ( $\sigma_{eg}^{(\dagger)}$ ) scattering from the electronic ground and excited state populations. The final two terms of Eq. (7) are due to scattering off coherences (we have used the fact that terms related by  $e \leftrightarrow g$  are complex conjugates to simplify). In contrast to the 1-molecule signal, the 2-molecule signal is given by the modulus square of an amplitude. The first two terms in this amplitude (Eq. (8)) correspond to the ground- and excited-state scattering amplitudes respectively while the final amplitude term is the scattering from coherences. We note that 2-molecule scattering from populations is purely elastic while 1-molecule scattering from populations contains both elastic and inelastic terms. In both cases, the presence of electronic coherences introduces new terms that result in heterodyne interference between transition charge densities and population charge densities, though the precise form of this contribution varies in the two cases.

The diffraction signal is commonly taken to be  $S \propto |\langle \hat{\sigma} \rangle|^2$ . This is correct for the 2-molecule contribution but does not generally hold for the 1-molecule contribution which is given by  $S_1 \propto \langle \hat{\sigma}^\dagger \hat{\sigma} \rangle$ . There are two important but subtle differences between these expressions: (1) heterodyne interference between ground- and excited-state scattering (i.e., terms of the form  $\sigma_{ee}\sigma_{gg}$ ) appear only in  $S_2$  and (2)  $S_2$  is proportional to  $\rho^2$  while  $S_1$  is linear in  $\rho$  so that the excited state diffraction  $\sigma_{ee}$  comes proportional to  $\rho_{ee}$  for  $S_1$  rather than  $\rho_{ee}^2$  for  $S_2$ . Since the 2-molecule contribution scales quadratically with the molecule number  $N$  at the Bragg peaks, this signal overwhelms the 1-molecule scattering there. In between the Bragg peaks, or in the absence of long-range order, the signal is governed by the 1-molecule scattering and should be calculated using Eq. (7) (note

the similarity to the discussion in Ref. [2], §3.1.3). The 1-molecule contribution is then linear in the molecular density matrix  $\rho$  and identified with Raman scattering while the 2-molecule is quadratic in  $\rho$  and corresponds to Rayleigh scattering [35]. While we are not the first to point out that diffraction from nonstationary states differs from a simple  $|\sigma(\mathbf{q})|^2$  form [3, 12, 36, 37], it is still widely employed. We suspect that the confusion on this point is exacerbated by a lack of clarity on the separation of terms into single- *vs.* two-molecule. While diffraction is often understood from an independent atom perspective and separated into single- and two-*atom* terms, this approach treats intermolecular and intramolecular structure on the same footing, as distances between atoms in the sample. Since the molecular structure is the quantity of interest and molecular bonding electrons are not independent, it is more appropriate and accurate to treat the inter- and intra-molecular structure separately as above. Moreover, our approach includes inelasticities, leading to transition charge densities  $\hat{\sigma}_{ij}(\mathbf{q})$  that are usually neglected but that interfere directly with ground and excited state terms  $\hat{\sigma}_{ii}(\mathbf{q})$ .

We demonstrate the relative magnitude of the different contributions to the single-molecule signal in Eq. 7, for sodium iodide. The two relevant valence states are the  $X^1\Sigma^+$  ground state and the  $A^1\Sigma^+$  state (referred to as  $g$  and  $e$  in the following). Figure 2 shows the difference density between  $\sigma_{gg}$  and  $\sigma_{ee}$  as well as the transition density  $\sigma_{ge}$ . The  $g \rightarrow e$  excitation is characterized by promoting an electron from  $n_{p_z}$  of the iodine into a  $\sigma^*$  bond, thus weakening the bond. This can be clearly seen in Fig. 2(a): electron density from in between the atoms and the lone pair at the iodine is removed. This feature is represented in similar way in the transition density (Fig. 2(b)).

In Fig. 3 the different contributions from the sum terms in Eq. 7 are shown for a fixed nuclear configuration ( $R = 2.5 \text{ \AA}$ ). Assuming an excitation fraction of 10% ( $\rho_{ee} = 0.1$ ), the strongest contribution to the  $S_1$  signal stems from the ground state density ( $\sigma_{gg}^2$ ) followed by the excited state density ( $\sigma_{ee}^2$ ), which is by one order of magnitude weaker (proportional to  $\rho_{ee}$ ). The diffrac-

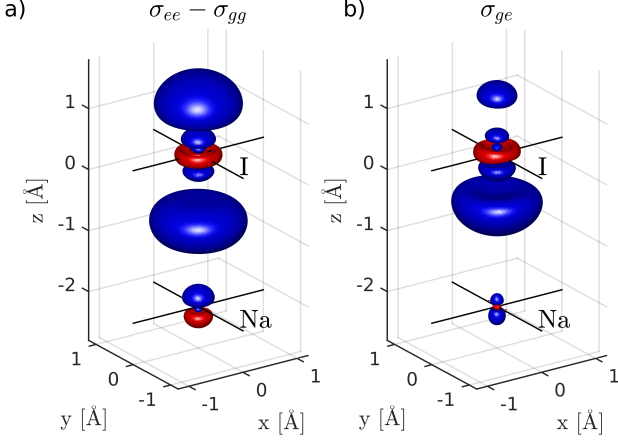


FIG. 2. Isosurfaces of the charge densities of NaI. The difference density (a)  $\sigma_{ee} - \sigma_{gg}$  and the transition density (b)  $\sigma_{ge}$  are evaluated for isovalues of 0.01 and 0.005 respectively (red: positive sign, blue: negative sign). The crosshairs mark the atomic centers.

tion pattern allows to directly determine bond length. In Fig. 3(c) the contribution which stems from valence electronic coherences ( $\rho_{ge}\sigma_{ee}^*\sigma_{ge}$ ) combined with inelastic X-ray scattering is shown for when the electronic coherence is maximal (e.g. directly after excitation with a pump). This contribution is  $\approx 3$ -4 orders of magnitudes weaker than the portion of the signal, which stems from  $\sigma_{ee}^2$  and is expected to rapidly decay as the nuclear wave packet leaves the Franck-Condon region. Contributions caused solely by the transition densities ( $\rho_{ge}\sigma_{ge}^2$ ) shown in Fig. 3(d), are  $\approx 6$  orders of magnitudes weaker than the excited state density contribution. This scaling behavior can be explained by the fact that diagonal densities ( $\rho_{ee}$  and  $\rho_{gg}$ ) are dominated by densely packed core electrons, while the transition densities are determined by  $\approx 1$  electron which is distributed over a valence orbital.

It becomes clear that  $\sigma_{ee}^2$  – assuming that the phase problem can be solved – is sufficient to qualitatively recover the nuclear wave packet motion in the excited state. This part contains solely the phase of the excited state nuclear wave packet. Given sufficiently short probe pulses (the pulse bandwidth must cover the energy gap between  $e$  and  $g$ ), the contributions from  $\rho_{ge}\sigma_{ee}^*\sigma_{ge}$  can potentially be retrieved. This, temporally fast oscillating, part of the signal contains the electronic phase information.

Ultrafast diffraction from photoexcited iodine in the gas phase was recently reported [1]. By taking the 2-molecule contribution to vanish (due to the lack of long-range order in the gas sample) while neglecting electronic coherences and inelastic scattering, Eq. (7) finally gives just an incoherent sum of scattering from each molecule  $S_1 \propto \rho_{ee}|\sigma_{ee}|^2 + \rho_{gg}|\sigma_{gg}|^2$ , i.e., the signal does look like that of a homogeneous mixture of excited and ground-

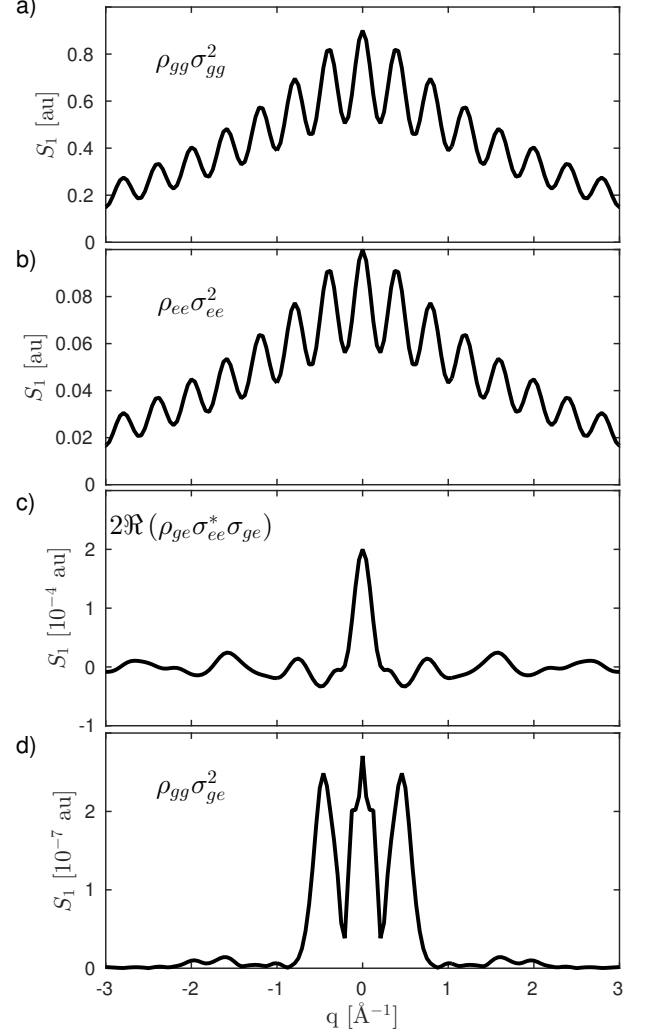


FIG. 3. Contributions to the single particle signal (see Eq. 7). The components of the signal show the projection onto the molecular axis and are normalized to  $\sigma_{gg}^2(0) = 1$ . The density matrix of the electronic states is given by  $\rho_{gg} = 0.9$ ,  $\rho_{ee} = 0.1$ ,  $\rho_{ge} = 0.3$ .

state molecules. We find no heterodyne  $\sim \sigma_{gg}\sigma_{ee}$  terms as claimed in Ref. [1]. Such terms do exist in time-resolved Bragg peaks in crystals, which is a 2-molecule signal, but are absent from the incoherent sum of single-molecule terms that characterizes gas-phase signals. We remark that the difference in the  $\rho$ -scaling between the single- and two-molecule terms is crucial: if the sample is perturbatively pumped so that some small percentage  $\rho_{ee}$  of molecules are in the excited state, 1-molecule scattering from the excited state is significantly stronger, compared to ground-state scattering, than it is in 2-molecule scattering ( $\rho_{ee}$  vs  $\rho_{ee}^2$  respectively). In fact, the 1-molecule excited-state scattering scales the same in  $\rho$  as the 2-molecule holographic interference that is the object of heterodyne detection, opening the door to

confusion. Experimentally sorting out the various terms in the diagrams in Fig. 1 will be an interesting future challenge. Finally, we note that homodyne versus heterodyne detection is a purely classical issue related to the macroscopic interference of light and has nothing to do with entanglement or Schroedinger cat states, as was incorrectly argued in Ref. [38]. Quantum features can only be created by electronic coherences which were neglected in Ref. [1].

The support of the Chemical Sciences, Geosciences, and Biosciences division, Office of Basic Energy Sciences, Office of Science, U.S. Department of Energy through award No. DE-FG02-04ER15571 as well as from the National Science Foundation (grant CHE-1361516) is gratefully acknowledged. Support for K.B. was provided by DOE. M.K. gratefully acknowledges support from the Alexander von Humboldt foundation through the Feodor Lynen program.

---

\* kcbennet@uci.edu

† smukamel@uci.edu

- [1] J. Glowina, A. Natan, J. Cryan, R. Hartsock, M. Kozina, M. Minitti, S. Nelson, J. Robinson, T. Sato, T. van Driel, *et al.*, *Phys. Rev. Lett.* **117**, 153003 (2016).
- [2] A. Guinier, *X-ray diffraction: in crystals, imperfect crystals, and amorphous bodies* (Courier Dover Publications, 1994).
- [3] J. Als-Nielsen and D. McMorrow, *Elements of modern X-ray physics* (Wiley, Hoboken, 2011).
- [4] P. Thibault and V. Elser, *Annu. Rev. Cond. Mat. Phys.* **1**, 237 (2010).
- [5] M. Ben-Nun, T. J. Martínez, P. M. Weber, and K. R. Wilson, *Chem. Phys. Lett.* **262**, 405 (1996).
- [6] B. J. Siwick, J. R. Dwyer, R. E. Jordan, and R. D. Miller, *Science* **302**, 1382 (2003).
- [7] R. C. Stevens, *Curr. Opin. Struct. Biol.* **10**, 558 (2000).
- [8] A. McPherson, *Crystallization of biological macromolecules* (Cold Spring Harbor Laboratory Press, 1999).
- [9] J. Hajdu, *Curr. Opin. Struct. Biol.* **10**, 569 (2000).
- [10] H. N. Chapman, *Nat. Mater.* **8**, 299 (2009).
- [11] D. Starodub, A. Aquila, S. Bajt, M. Barthelmess, A. Barty, C. Bostedt, J. Bozek, N. Coppola, R. Doak, S. Epp, *et al.*, *Nat. Commun.* **3**, 1276 (2012).
- [12] S. Bratos, F. Mirloup, R. Vuilleumier, and M. Wulff, *J. Chem. Phys.* **116**, 10615 (2002).
- [13] P. Coppens, I. I. Vorontsov, T. Graber, M. Gembicky, and A. Y. Kovalevsky, *Acta Crystallographica Section A: Foundations of Crystallography* **61**, 162 (2005).
- [14] H. Ihee, M. Lorenc, T. K. Kim, Q. Y. Kong, M. Cammarata, J. H. Lee, S. Bratos, and M. Wulff, *Science* **309**, 1223 (2005).
- [15] M. Wulff, S. Bratos, A. Plech, R. Vuilleumier, F. Mirloup, M. Lorenc, Q. Kong, and H. Ihee, *J. Chem. Phys.* **124**, 034501 (2006).
- [16] M. Cammarata, M. Levantino, F. Schotte, P. A. Anfinrud, F. Ewald, J. Choi, A. Cupane, M. Wulff, and H. Ihee, *Nature methods* **5**, 881 (2008).
- [17] C. W. Siders, A. Cavalleri, K. Sokolowski-Tinten, C. Tth, T. Guo, M. Kammler, M. H. v. Hoegen, K. R. Wilson, D. v. d. Linde, and C. P. J. Barty, *Science* **286**, 1340 (1999).
- [18] M. Woerner, F. Zamponi, Z. Ansari, J. Dreyer, B. Freyer, M. Prémont-Schwarz, and T. Elsaesser, *J. Chem. Phys.* **133**, 064509 (2010).
- [19] P. Coppens, *J. Phys. Chem. Lett.* **2**, 616 (2011).
- [20] R. Neutze and K. Moffat, *Current opinion in structural biology* **22**, 651 (2012).
- [21] J. Larsson, R. W. Falcone, *et al.*, *Appl. Phys. A Mater. Sci. Process.* **66**, 587 (1998).
- [22] M. Altarelli *et al.*, Technical Design Report, DESY **97** (2006).
- [23] J. Feldhaus, J. Arthur, and J. B. Hastings, *J. Phys. B-At. Mol. Opt.* **38**, S799 (2005).
- [24] B. W. J. McNeil and N. R. Thompson, *Nat. Photon.* **4**, 814 (2010).
- [25] H. N. Chapman, P. Fromme, A. Barty, T. A. White, R. A. Kirian, A. Aquila, M. S. Hunter, J. Schulz, D. P. DePonte, and U. Weierstall, *Nature* **470**, 73 (2011).
- [26] C. Bostedt, J. Bozek, P. Bucksbaum, R. Coffee, J. Hastings, Z. Huang, R. Lee, S. Schorb, J. Corlett, P. Denes, *et al.*, *Journal of Physics B: Atomic, Molecular and Optical Physics* **46**, 164003 (2013).
- [27] A. Barty, J. Küpper, and H. N. Chapman, *Annual review of physical chemistry* **64**, 415 (2013).
- [28] M. J. Vrakking and T. Elsaesser, *Nature Photonics* **6**, 645 (2012).
- [29] M. Woerner, F. Zamponi, Z. Ansari, J. Dreyer, B. Freyer, M. Prémont-Schwarz, and T. Elsaesser, *The Journal of Chemical Physics* **133**, 064509 (2010), <http://dx.doi.org/10.1063/1.3469779>.
- [30] K. Bennett, J. D. Biggs, Y. Zhang, K. E. Dorfman, and S. Mukamel, *J. Chem. Phys.* **140**, 204311 (2014).
- [31] Since the 2-molecule contributions carry spatial phase-factors that require long-range coherent order to observe, they had been termed coherent in Ref. [30]. The single-molecule contributions on the other hand were termed incoherent since they add incoherently for the total signal. Nonetheless, the 1-molecule contribution still has intramolecular spatial coherences (between atoms) so for clarity we use in this work the terms 1- and 2-molecule rather than incoherent and coherent.
- [32] J. Miao, P. Charalambous, J. Kirz, and D. Sayre, *Nature* **400**, 342 (1999).
- [33] I. K. Robinson, I. A. Vartanyants, G. Williams, M. Pfeifer, and J. Pitney, *Phys. Rev. Lett.* **87**, 195505 (2001).
- [34] J. Miao, T. Ishikawa, E. H. Anderson, and K. O. Hodgson, *Phys. Rev. B* **67**, 174104 (2003).
- [35] K. E. Dorfman, K. Bennett, Y. Zhang, and S. Mukamel, *Phys. Rev. A* **87**, 053826 (2013).
- [36] W. Schulke, *Electron dynamics by inelastic X-ray scattering* (Oxford University Press, Oxford; New York, 2007).
- [37] G. Dixit, O. Vendrell, and R. Santra, *Proc. Natl. Acad. Sci.* **109**, 11636 (2012).
- [38] “SLAC, press release archive,” <https://goo.gl/d8FMP2>, accessed: 2016-11-17.